

Time Domain Simulations of the Behaviour of Fast Ships in Oblique Seas

Frans van Walree

Maritime Research Institute Netherlands, THE NETHERLANDS

Pepijn de Jong

*Ship Hydromechanics Laboratory, Delft University of Technology,
THE NETHERLANDS*

ABSTRACT

The fundamentals of a time domain seakeeping code (PANSHIP) are presented. Although the formulations enable a non-linear treatment of the submerged hull form, partial linearization is required for computational efficiency. The seakeeping code is applied to a high speed trimaran operating in oblique seas and calculation results are compared with experimental data.

KEYWORDS

Time domain panel code, seakeeping, course keeping, high speed trimaran, dynamic (in)stability.

INTRODUCTION

The continuous demand for high speed operation while fulfilling existing and extended operational and mission requirements has become a constant challenge for the naval architect. There is a perpetual competition in the industry to develop innovative methods of reducing resistance and expanding maximum speeds in a seaway.

Evaluation of advanced and/or high speed concepts requires advanced numerical tools that can deal with the hydrodynamic issues involved on a first principles basis. Investigations are not limited to issues like linear motion induced accelerations in the vertical plane, but need to address slamming, whipping, fatigue damage, course keeping and dynamic stability as well.

The present paper discusses a numerical method that can be applied to (high speed) hull

forms. The method is at present limited to non-linear motions including course keeping and dynamic stability. Simulation results are shown for a high speed trimaran and illustrate the application and validity of the method.

NUMERICAL FORMULATION

The numerical method is an extension of the work presented by Lin and Yue (1990), Pinkster (1998) and Van Walree (2002). The PANSHIP code contains the numerical method.

Time domain Green function method

Potential flow is assumed based on the following simplifications of the fluid. It is assumed to be:

- homogeneous,
- incompressible,
- without surface tension,

- inviscid and irrotational.

The medium of interest is water, while there is an interface with air. The ambient pressure is assumed to equal zero. The water depth is infinite and waves from arbitrary directions are present. Under these assumptions it can be shown that the Laplace equation, resulting from conservation of mass, is valid in the interior of the fluid:

$$\nabla^2 \Phi = 0 \quad (1)$$

The following definitions are used to describe the domain:

- $V(t)$ is the fluid volume, bounded by:
- $S_F(t)$ the free surface of the fluid,
- $S_H(t)$ the submerged part of the hull of the ship,
- $S_L(t)$ lifting surfaces,
- $S_W(t)$ wake sheets and
- $S_\infty(t)$ the surface bounding the fluid infinitely far from the body.
- The total potential can be split into two parts, the wave potential and the disturbance potential:

$$\Phi = \Phi^w + \Phi^d \quad (2)$$

The wave potential is given by:

$$\Phi^w = \frac{\zeta_a}{\omega} e^{kz} \sin(k(x_0 \cos \psi + y_0 \sin \psi) - \omega t) \quad (3)$$

The subscript ‘0’ refers to earth fixed coordinates. At the free surface two conditions are imposed. First, a kinematic condition assuring that the velocity of a particle at the free surface is equal to the velocity of the free surface itself:

$$\frac{\partial \eta}{\partial t} + \nabla \Phi \cdot \nabla \eta - \frac{\partial z_0}{\partial t} = 0 \quad \forall \vec{x}_0 \in S_F \quad (4)$$

Second, a dynamic condition assuring that the pressure at the free surface is equal to the ambient pressure. For this condition use is made of the unsteady Bernoulli equation in a translating coordinate system:

$$\frac{\partial \Phi}{\partial t} + g\eta + \frac{1}{2}(\nabla \Phi)^2 = 0 \quad \forall \vec{x}_0 \in S_F \quad (4)$$

Both can be combined and linearized around the still water free surface, yielding:

$$\frac{\partial^2 \Phi}{\partial t^2} + g \frac{\partial z_0}{\partial t} = 0 \quad \text{at } z_0 = 0 \quad (6)$$

On the instantaneous body surface a zero normal flow condition is imposed by setting the instantaneous normal velocity of the body equal to:

$$V_n = \frac{\partial \Phi^d}{\partial n} + \frac{\partial \Phi^w}{\partial n} \quad \forall \vec{x}_0 \in S_{HL}(t) \quad (5)$$

At a large distance from the body the influence of the disturbance is required to vanish:

$$\Phi_d \rightarrow 0 \quad \frac{\partial \Phi^d}{\partial t} \rightarrow 0 \quad \text{when } r \rightarrow S_\infty \quad (6)$$

At the start of the process, apart from the incoming waves, the fluid is at rest, as is reflected in the initial condition.

$$\Phi_d \Big|_{t=0} = \frac{\partial \Phi^d}{\partial t} \Big|_{t=0} = 0 \quad (7)$$

In this time-domain code the Green function given in equation (8) will be used. This Green function specifies the influence of a singularity with impulsive strength (submerged source or doublet) located at singularity point q (ξ, η, ζ) on the potential at field point p (x_0, y_0, z_0).

$$G(p, t, q, \tau) = G^0 + G^f = \frac{1}{R} - \frac{1}{R_0} + 2 \int_0^\infty \left[1 - \cos(\sqrt{gk}(t - \tau)) \right] e^{k(z_0 + \zeta)} J_0(kr) dk$$

for $p \neq q, t \geq \tau$

where

$$R = \sqrt{(x_0 - \xi)^2 + (y_0 - \eta)^2 + (z_0 - \zeta)^2}$$

$$R_0 = \sqrt{(x_0 - \xi)^2 + (y_0 - \eta)^2 + (z_0 + \zeta)^2}$$

$$r = \sqrt{(x_0 - \xi)^2 + (y_0 - \eta)^2}$$

(8)

In equation (8):

- the G^0 -term is the source and doublet plus biplane image part (or Rankine part), while
- the G^f -term is the free surface memory part of the Green's function, and
- J_0 is the Bessel function of order zero, t is time while τ is the past time.

It has been shown, by for example Pinkster (1998), that the Green function satisfies both the Laplace equation and the boundary conditions, making it a valid solution for the boundary value problem stated above.

Using the above, it is possible to derive a boundary integral formulation. The first step is to apply Green's second identity to:

$$\Phi^d(\vec{x}_0, t) \text{ and } \partial G / \partial \tau(\vec{x}_0, \vec{\xi}, t - \tau) \quad (9)$$

Next, the free surface integral is eliminated by virtue of the Green function. Finally, a general formulation of the nonlinear integral equation is obtained for any field point:

$$4\pi T \Phi^d(p, t) = - \int_{S_{HLW}(t)} (\Phi^d G_n^0 - G^0 \Phi_n^d) dS + \int_0^t d\tau \int_{S_{HLW}(\tau)} (\Phi^d G_{\tau n} - G_\tau \Phi_n^d) dS + \frac{1}{g} \int_0^t d\tau \int_{C(\tau)} (\Phi^d G_{\tau\tau} - G_\tau \Phi_\tau^d) V_N dS \quad (10)$$

V_N is the projection of the normal velocity at the curve C in the plane of the free surface, for example $G_n^0 = \partial G^0 / \partial n$ etc., and T is defined as:

$$T(p) = \begin{cases} 1 & p \in V(t) \\ 1/2 & p \in S_H(t)N \\ 0 & \text{otherwise} \end{cases} \quad (11)$$

A source distribution will be present on the body surface and a combined source-doublet distribution on lifting surfaces. The source strength is set equal to the jump in the normal derivative of the potential between the inner and outer sides of the surface, while the doublet strength is set equal to the jump of the potential across the inner and outer surfaces.

Using such source and doublet distributions finally results in the principal equation to be

solved for the unknown singularity strengths:

$$4\pi \left(V_{n_p} - \frac{\partial \Phi^w}{\partial n_p} \right) = 2\pi \sigma_p + \int_{S_{HLW}(t)} \sigma(q, t) \frac{\partial G^0}{\partial n_p} dS + \int_{S_{HLW}(t)} \mu(q, t) \frac{\partial^2 G^0}{\partial n_p \partial n_q} dS - \int_0^t d\tau \int_{S_{HLW}(\tau)} \sigma(q, t) \frac{\partial^2 G^f}{\partial t \partial n_p} dS - \int_0^t d\tau \int_{S_{HLW}(\tau)} \mu(q, t) \frac{\partial^3 G^f}{\partial t \partial n_p \partial n_q} dS - \frac{1}{g} \int_0^t d\tau \int_{L_w(\tau)} \sigma(q, t) \frac{\partial^2 G^f}{\partial t \partial n_p} V_N V_n dL \quad (12)$$

In this equation a subscript p of n indicates a normal derivative at the field point p and subscript q at singularity point q . V_n is the normal velocity at the collocation point.

A wake model is necessary for an unique solution of equation (12). The wake model relates the dipole strength at the trailing edge of lifting surfaces to the location and shape of a wake sheet, in order to both satisfy the Kutta condition and Kelvin's circulation.

These requirements are satisfied by transferring the net circulation at the trailing edge into the adjacent wake sheet elements. For the wake sheets the doublet elements are replaced by equivalent vortex ring elements as a discretization of the continuous vortex sheet. The sum of the circulation strengths along each individual vortex ring segment is always zero, as detailed in Katz and Plotkin (2001).

A further requirement is that the wake sheet should be force free. It is not a solid surface, so no pressure difference can be present between the upper and lower sides of the sheet. The force on a vortex sheet is given by the Kutta-Joukowski law:

$$\vec{F} = \rho \vec{V} \times \gamma \quad (13)$$

From this law can be determined that for zero force the vorticity vector should be directed

parallel to the velocity vector. This can be accomplished by displacing the vortex element corner points with the local fluid velocity. However, a reduction of the computational effort is achieved by prescribing the wake sheet position and form. This prescription is simply, that a wake element remains stationary once shed. This eliminates the effort needed to calculate the exact position of each wake element at each time step. This violates the requirement of a force free wake sheet. However, for practical purposes this does not have significant influence as shown by Van Walree (1999) and Katz and Plotkin (2001).

The equation is discretized in terms of a source element distribution on the hull, a doublet element discretization on the lifting surfaces and equivalent vortex ring elements on the wake surface. In the current method constant strength quadrilateral source and doublet panels are used. This leads to the discretized form of equation (12).

At the start of the simulation the body is impulsively set into motion. At each subsequent time step the body is advanced to a new position with an instantaneous velocity. Both position and velocity are known from the solution of the equation of motion. The discretized form of equation (12) is solved to obtain the singularity strength at each time step.

Linearization

Especially the evaluation of the free surface memory term of the Green's function requires a large amount of computational time. These terms need to be evaluated for each control point for the entire time history at each time step. To decrease this computational burden, the evaluation of the memory term has been simplified. For near time history use is made of interpolation of predetermined tabular values for the memory term derivatives, while for larger values further away in history polynomials and asymptotic expansion are

used to approximate the Green function derivatives.

Moreover, the position of the hull and lifting surfaces relative to the past time panels is not constant due to the unsteady motions, making recalculation of the influence of past time panels necessary for the entire time history. This recalculation results in a computational burden requiring the use of a supercomputer. To avoid this burden, the unsteady position of hull and lifting surfaces is linearized to the average position (moving with the constant forward speed). Now the memory integral can be calculated a priori for use at each time step during the simulation.

The prescription of the wake sheets in this linear approach leads to a flat wake sheet behind the lifting surface. Again a constant distance exist to the past time wake panels. Only the influence coefficients of the first row of wake elements need to be calculated at each time step, until the maximum wake sheet length is reached. For all other rows the induced velocity can be obtained by multiplying the influence by their actual circulation.

Force evaluation

Forces can be obtained from integration of the pressure at each collocation point over the body. The pressures can be obtained by using the unsteady Bernoulli equation (in a body fixed axis system):

$$\frac{p_a - p}{\rho} = \frac{1}{2} \left\{ \left(\frac{\partial \Phi}{\partial x} \right)^2 + \left(\frac{\partial \Phi}{\partial y} \right)^2 + \left(\frac{\partial \Phi}{\partial z} \right)^2 \right\} + \frac{\partial \Phi}{\partial t} - \vec{V} \cdot \nabla \Phi + gz \quad (14)$$

In equation (14) \vec{V} is the total velocity vector at the collocation point of the rigid body, including rotations.

The spatial derivatives of the potential in equation (14) follow from the solution. The only difficulty remaining is to obtain the time derivative. For the contribution of the wake

and the Rankine part of the doublet panels this can be done by utilizing a straightforward backward difference scheme. However, this gives unstable results when used for the contribution of the source panels and the memory part of the doublet panels to the time derivative. This instability is solved by calculating the time derivative of these contributions analytically from the Green function derivatives.

This means that additional Green function derivatives have to be obtained, besides the derivatives needed for the solution itself. Furthermore, the time derivative of the source strength is needed. One solution is to derive this derivative directly from the solution itself:

$$\begin{aligned}\sigma &= A^{-1}v_n \\ \frac{\partial\sigma}{\partial t} &= A^{-1} \frac{\partial v_n}{\partial t}\end{aligned}\quad (15)$$

In this equation A is the solution matrix relating the singularity strengths via the Rankine influences to the RHS. The vector v_n is the RHS vector of the solution, containing all influences due to incident wave, free surface memory effects and rigid body motions in terms of normal velocity in the collocation points. To obtain the time derivative of the free surface memory part of this vector, again extra Green function derivatives need to be obtained. The time derivative of the wave contributions can be obtained analytically. The time derivative of the rigid body velocity is the rigid body acceleration. This acceleration is multiplied by the inverse of the Rankine influence matrix that equals the added mass. This contribution can be transferred to the mass times acceleration part of the equation of motion.

Ventilated transom sterns

Methods using a transient Green function are not able to deal with ventilated transom sterns. To compensate for this two measures can be taken:

- Add a dummy section at the transom that

ensures flow alignment. Do not take into account the forces acting on such a segment on the body. This dummy segment avoids the occurrence of unrealistically high velocities around the transom.

- Another measure that can be taken is to set the pressure to atmospheric at the transom by applying a smooth function over a certain length from the transom that reduces the pressure accordingly.

Inclusion of viscous flow effects

With respect to the viscous resistance R_v , empirical formulations are applied to each part separately (hull, outriggers, lifting surfaces). The formulations used can be generalised as follows:

$$\begin{aligned}R_v &= \frac{1}{2} \rho U^2 S (1 + k) C_F \\ C_F &= \frac{0.075}{(\log_{10}(R_n) - 2)^2}\end{aligned}\quad (18)$$

where U is the ship speed, S is the wetted surface area, k is a suitable form factor, and R_n is the Reynolds number of the body part considered.

Viscous damping

For high speed vessels, having only slight potential damping, viscous damping can play an important role. This is especially true around peak motion response frequencies. The magnitude of these forces depends on oscillation frequency, Froude number and section shape. In the current model a cross flow analogy is used to account for these forces. The viscous damping coefficient only depends on section shape, other influences are neglected. The following formulation is used in a strip wise manner:

$$F = -\frac{1}{2} \rho |V_r| V_r S C_D \quad (19)$$

V_r is the sectional relative velocity with respect to the flow, while S is either the horizontal or vertical projection of the section

area. The cross-flow drag coefficient C_D has values in-between 0.25 and 0.80.

This formulation is applied for both the vertical and horizontal plane motions. High speed ships have generally slender hull forms so that flow separation due low frequency motions in the horizontal plane is assumed to be insignificant and a relatively simple formulation such as equation (19) can be used..

An additional term is incorporated for the hull roll damping K_p :

$$K_p = -(b_p p + b_{pp} |p| p) \quad (20)$$

where p is the roll velocity and b_p and b_{pp} are linear and quadratic roll damping coefficients respectively, determined by means of MARIN's FDS method, see Blok and Aalbers (1991).

Ride control system

A ride control algorithm is included in the code actuating control surface settings. The basic equation is:

$$\ddot{\delta} = P(\ddot{x}_r - \ddot{x}_s) + D(\dot{\ddot{x}}_r - \dot{\ddot{x}}_s) + A(\ddot{\ddot{x}}_r - \ddot{\ddot{x}}_s) \quad (21)$$

where $\ddot{\delta}$ is the control surface deflection; P , D , and A are proportional, damping and acceleration coefficients respectively; and \ddot{x}_r and \ddot{x}_s are the required and actual motion vectors respectively; and an overdot denotes differentiation with respect to time. Equation (21) is used for both the ride control and the auto pilot systems.

Propulsion and steering

A propulsion and steering system for water jets is included. The formulations are based on captive model tests on several types of high speed craft and read as follows for the side force and yaw moment, Y_w and N_w respectively:

$$Y_w = \rho(T_{nn}n^2 + T_{Un}Un) \sin(F_\delta \delta) \quad (22)$$

$$N_w = \rho(T_{nn}n^2 + T_{Un}Un) \sin(F_\delta \delta) x_\delta$$

where T is a thrust coefficient, U is forward speed, n is the RPM and F_δ is an empirical coefficient.

APPLICATION AND VALIDATION

One case will be discussed here. It concerns a high speed trimaran design operating in oblique irregular seas. The main particulars of the vessel are shown in Table 1 while Figure 1 shows the model in the Seakeeping and Manoeuvring Basin of MARIN during a run in 5.5 m stern quartering seas.

Table 1. General characteristics of the Trimaran

Length Lpp	110.00 m
Beam	26.40 m
Draft	4.60 m
Displacement	2310 tons
Design speed	45 kt
GM	1.70 m

An interesting feature of the vessel is that it suffers from a dynamic instability in heel, especially at higher speeds. Figure 2 shows the calculated pressure distribution on the submerged outrigger hull portion for a speed of 45 kt and a heel angle of 10 deg. The low pressures result in a suction force which tends to reduce the restoring moment to about zero.



Figure 1 Trimaran model in the SMB

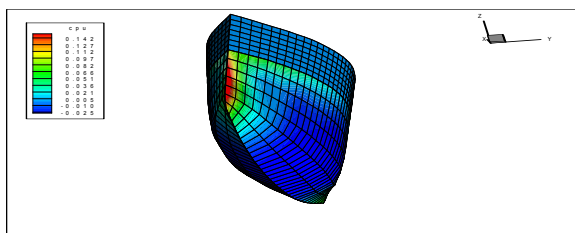


Figure 2 Pressure distribution on outrigger at 10 deg heel and 45 kt speed

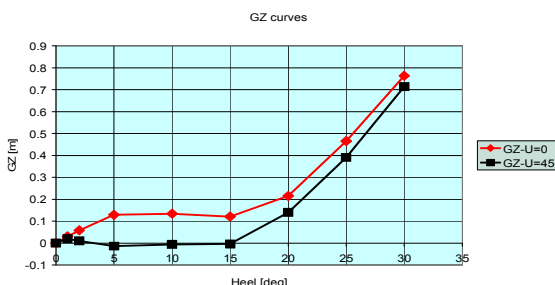


Figure 3 GZ curves at zero speed and at 45 kt.

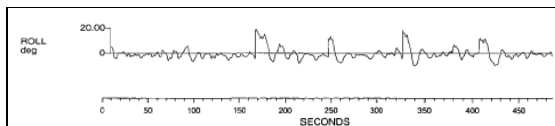


Figure 4 Experimental roll time trace at 45 kt and 135 deg heading.

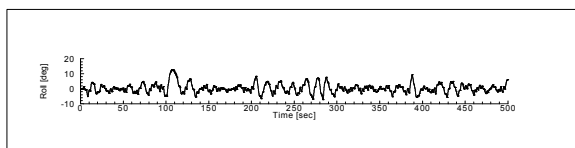


Figure 5 Calculated roll time trace at 45 kt and 135 deg heading.

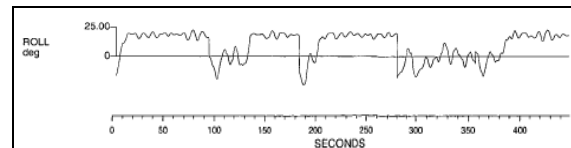


Figure 6 Experimental roll time trace at 45 kt and 45 deg heading.

The GZ curves at rest and at a 45 kt speed are shown in Figure 3. Both curves are based on calm water PANSIP simulations whereby the vessel was fixed in all modes of motion. Similar results have been obtained for a range of speeds and have been stored in the linear mode code as a hydrodynamic correction on the restoring moment. At heel angles above 20 degrees the deck connecting the outriggers to the hull gets submerged and greatly increases the static stability which makes the vessel virtually impossible to capsize.

Figures 4 through 7 show parts of the experimental and simulated time traces for roll at a 45 kt speed in an irregular sea with a 2.5 m significant wave height, for wave directions of 135 (bow quartering) and 45 (stern quartering) degrees respectively. For bow quartering seas the signals show isolated large roll excursions, for stern quartering seas alternating large mean heel angles occur. Although the actual wave trains in the simulations are different from these in the experiments, the general behavior is well captured by the simulations.

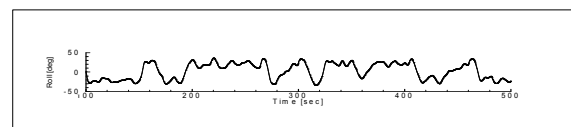


Figure 7 Calculated roll time trace at 45 kt and 45 deg heading.

Further statistical comparisons for heave, roll, pitch and yaw motions are given in Figures 8 through 14 for conditions as specified in Table 2. A 0 degree wave direction means following waves while a 180 deg wave direction means bow waves. For all tests, at least 180 wave encounters were recorded.

Table 2 Test conditions

Test	Speed [kt]	Wave direction [deg]	Significant wave height [m]	Peak period [sec]
1	25	90	5.5	9.5
2	25	45	5.5	9.5
3	25	15	5.5	9.5
4	25	60	5.5	9.5
5	45	135	2.5	7.0
6	45	90	2.5	7.0
7	45	45	2.5	7.0

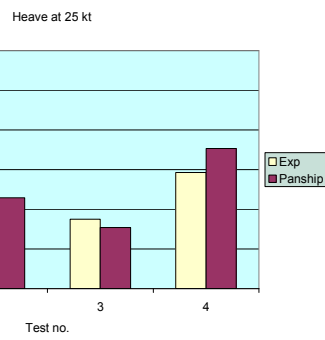


Figure 8 Comparison heave response at 25 kt

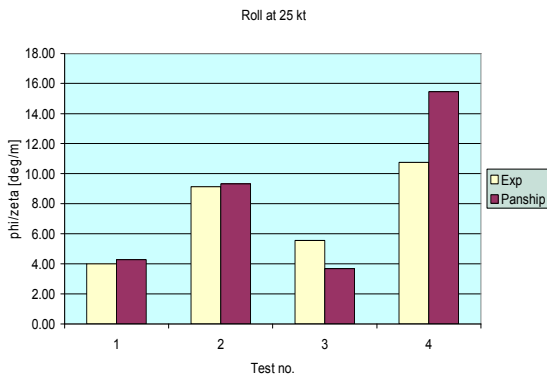


Figure 9 Comparison roll response at 25 kt

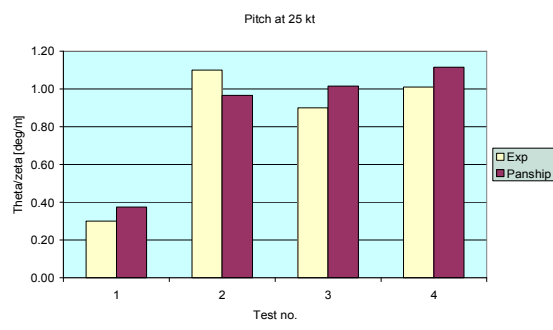


Figure 10 Comparison pitch response at 25 kt

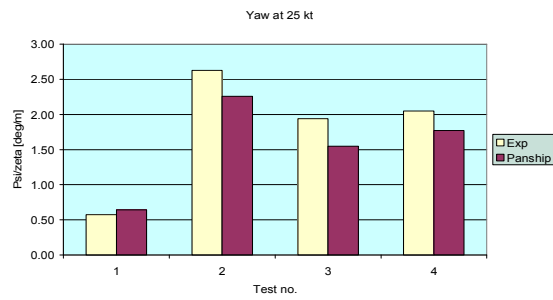


Figure 11 Comparison yaw response at 25 kt

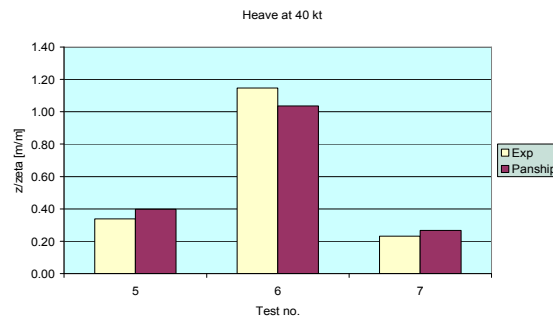


Figure 12 Comparison heave response at 40 kt

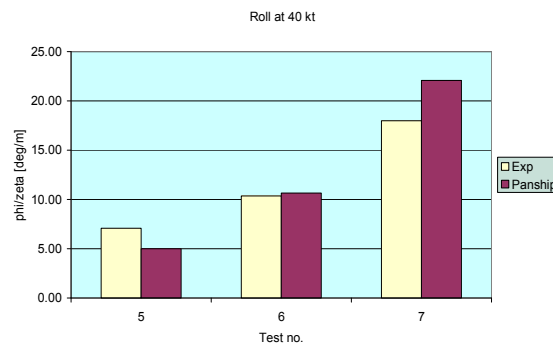


Figure 13 Comparison roll response at 45 kt

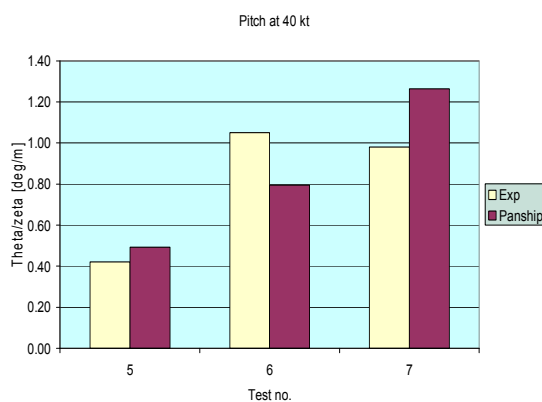


Figure 14 Comparison pitch response at 45 kt

Heave and pitch are quite well predicted for both speeds, indicating that the method deals well with non-linear effects due to large (roll) motions.

The roll prediction for the 25 kt speed is quite acceptable for tests 1 through 3, but deviates from the experimental value for test 4. For the 45 kt speed, the roll is reasonably good in agreement with the experiments. Yaw is well predicted for both speeds.

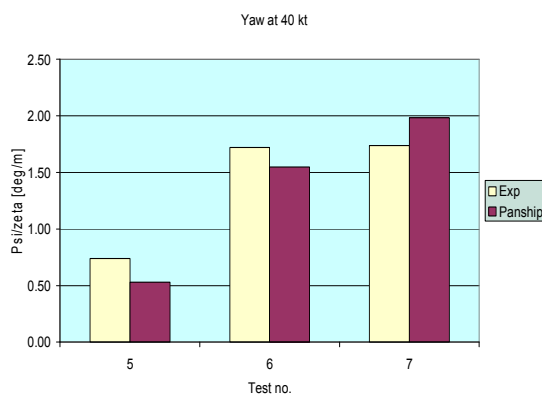


Figure 15 Comparison yaw response at 45 kt

Overall, in view of the highly non-linear behavior of the Trimaran in roll, these predictions are thought to be quite satisfactory.

CONCLUSIONS AND RECOMMENDATIONS

A time domain panel method for prediction of the dynamic behavior of (high speed) unconventional hull forms in waves is presented.

Simulation results are presented and compared to experimental results for a Trimaran with a dynamic stability problem. Predictions for vertical plane motions are generally quite good. Despite the use of a relatively simple method for viscous flow damping, predictions for horizontal plane motions are deemed acceptable.

It is anticipated that through the treatment of the hull form as a lifting surface even better predictions for both vertical and horizontal plane motions can be obtained in the future, and the use of empirical “viscous flow coefficients” can be reduced. Research into this topic is underway.

ACKNOWLEDGEMENTS

The permission from Naval Sea Systems Command USA to publish the experimental data on the Trimaran is gratefully acknowledged.

REFERENCES

- Blok J.J. and Aalbers A.B., “Roll Damping Due to Lift Effects on High Speed Monohulls”, Proceedings FAST’91 Conference, Vol 2, pp 1331, 1991.
- Jong, P. de, Walree, F. van, Keuning, J.A., Huijsmans, R.H.M., “Evaluation of the free surface elevation in a time-domain panel method for the seakeeping of high speed ships”. Proceedings of the Seventeenth Int. Offshore and Polar Engineering Conference, Lisbon, 2007.
- Katz J. and Plotkin, A., “Low-speed Aerodynamics”, Cambridge University Press, Second Edition 2001.
- Lin, W. M. and Yue, D., “Numerical solutions for large-amplitude ship motions in the time domain”, Proceedings of the 18th Symposium on Naval Hydromechanics, Ann Arbor, pp. 41–65, 1990.

Proceedings of the 10th International Ship Stability Workshop

Pinkster, H.J.M., "Three dimensional time domain analysis of fin stabilized ships in waves". Master's thesis, Delft University of Technology, Department of Applied Mathematics, 1998.

Walree, F. van, "Computational methods for hydrofoil craft in steady and unsteady flow", PhD thesis, Delft University of Technology, 1999.

Walree, F. van, "Development, validation and application of a time domain seakeeping method for high speed craft with a ride control system". Proceedings of the 24th Symposium on Naval Hydrodynamics, pp. 475-490, 200